JOURNAL OF GEOPHYSICAL RESEARCH, VOL. 102, NO. A7, PAGES 14,625–14,630, JULY 1, 1997

Alfvén wave far field from steady-current tethers

Juan R. Sanmartín

Escuela Técnica Superior de Ingenieros Aeronáuticos, Universidad Politécnica de Madrid

Robert D. Estes

Harvard-Smithsonian Center for Astrophysics, Cambridge, Massachusetts

Abstract. We analyze the Alfvén wave signature left behind in the ionosphere by orbiting insulated tethers operating as thrusters or generators with steady currents. Using a recent description of tether radiation to determine the far field, we show that, at their leading edges, the Alfvén wings have an Airy function crosswise structure. The field amplitude falls off weakly as the inverse cube root of the distance along the wave front. The front itself, which carries a negligible fraction of the power radiated as Alfven waves, broadens proportionally to the cube root of that distance. We show that collisional decay becomes important at about 10^3 km along the front. For tethers longer than about 2 km, the top and bottom structures ("wings") are fully disjoint.

Introduction

In addition to their potential uses in space applications, current-carrying tethers in Earth orbit provide unique active experiments in ionospheric wave excitation. A review paper by *Dobrowolny and Melchioni* [1993] examines this and other aspects of tethered system electrodynamics and may be referred to for a thorough list of references to previous theoretical and experimental work. In the standard picture of a tethered satellite system that has a steady electrical current flowing through it by means of continual charge exchange with the ambient plasma, "circuit closure" is accomplished by charge-carrying electromagnetic waves excited in the ionosphere by the passage of the system. The dual constraints of steady state operation (Döppler condition) and satisfaction of the plasma wave dispersion relation are quite stringent and, as demonstrated by *Barnett and Olbert* [1986], greatly restrict the types and frequency ranges of waves available for circuit closure. We note in particular that whistler waves, which have been observed in plasma chamber experiments meant to model the operation of a tethered system [*Stenzel and Urrutia*, 1990], do not satisfy the criteria for propagating waves from a constant-current tether orbiting the Earth [*Sanmartín and Martinez-Sanchez*, 1995].

Among the propagating waves that can be excited by a constant-current tether are those lying on the Alfvén branch with frequencies below the ion cyclotron frequency. Alfvén wave packets associated with the motion of a large conductor moving through a magnetoplasma and which serve to carry current in the ionospheric transmission line, completing the electrical circuit that includes the moving conductor, were first described theoretically by *Drell et al.* [1965]. Since then a number of authors [*Estes*, 1988; *Rasmussen et al.*, 1990; *Donahue et al.*, 1991; *Lüttgen and Neubauer*, 1994], in addition to those previously cited, have considered the so-called "Alfvén wings" with particular application to tethered systems in space.

Ground-based measurements of electromagnetic signals associated with tether-induced ionospheric waves have been attempted during the Plasma Motor Generator (PMG) experiment and the Tethered Satellite System 1 Reflight (TSS-1R) experiment in which a 20-km-long tether was deployed from the U.S. Space Shuttle in February 1996, attaining currents of over 1 A. Unfortunately, there were no properly equipped and positioned satellites available to measure waves from TSS-1R in the ionosphere. However, tether systems have been proposed to supply magnetic reboost and power generation to the International Space Station, and such systems might be of similar use in the outer planets. It is thus desirable to have a good theoretical representation of the plasma waves associated with tether currents hundreds of kilometers from the system to guide the planning of data collection and analysis, which could, in turn, help validate the theory.

The present work is a step in that direction. We obtain far-field values of the Alfvén wing field components and the general shape of these wing structures. *Rasmussen et al.* [1990] have derived asymptotic approximations to that part of the wings well behind the front, and we compare our corresponding results to theirs below. *McKenzie et al.* [1993] used a nondispersive MHD model to study the far field and thus missed the complex structure described here. We also discuss collisional effects and the possible overlap of the top and bottom wings.

Far-Field Formulation

We consider a standard tethered-satellite system, orbiting in a magnetized plasma and consisting of an insulated, conducting tether with terminating contactors, where we use the term generically to include metallic surfaces in electrical contact with the tether and exposed to the ambient plasma as well as plasma devices such as hollow cathodes which define the regions of charge exchange between the tethered system and the ionosphere. In our calculations we first use collisionless, cold-plasma theory and assume an infinite, uniform ionosphere and a constant background magnetic field. Motion of the system is taken to be linear with a constant speed. The geomagnetic field is perpendicular to the system's velocity vector, but it is allowed to tilt at an arbitrary angle with respect to the horizontal. (See Figure1.) The tether is vertical.

Results apply equally to a system operating in the thruster or generator mode. We are not studying transient effects that may occur when the tether is first "turned on," for example, when current

Paper number 97JA00346.
0148-0227/97/97JA-00346$09.00

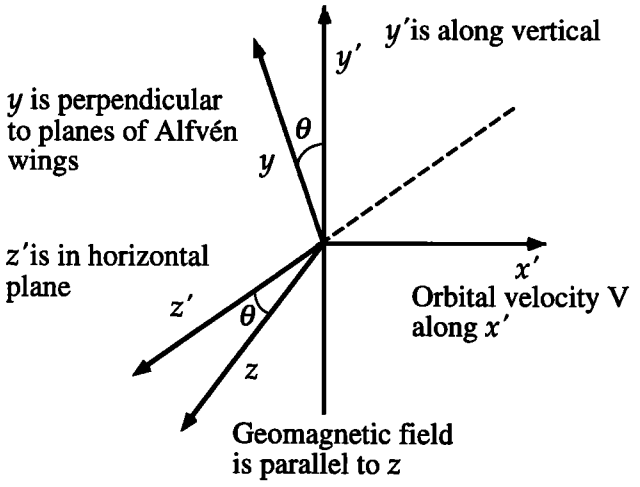

Figure 1. Coordinate systems used in the analysis. Origin is at the center of the vertical tether.

flow is activated by closing a switch; rather, we assume that a steady state has been reached in which a constant current is flowing in the tether with charge exchange taking place between the system and the ionosphere through the terminating contactors. This implies that the plasma has adjusted to the presence of the tethered system so that currents and fields measured in the system or the plasma are constant in time at any point fixed in the rest frame of the tether.

Thus, in the tether rest frame an observer sees a steady "structure" of fields and currents extending indefinitely into the plasma. The situation is rather like an idealized version of the bow wave of a boat, which appears unvarying when viewed from the boat. From the standpoint of the plasma, things seem far more dynamic. As the tether approaches, plasma upstream from the system begins to feel the effects of the tethered system's perturbation in the form of the fields and currents induced in the plasma closer to the system. At a given point in the plasma rest frame the fields and currents will vary (markedly for a point near the track of one of the terminating contactors) as the system passes by.

Plasma wave phenomena are conveniently analyzed by considering the plasma to be a dielectric medium. The plasma current is incorporated into the displacement current terms of Maxwell's equations. Wave equations can then be derived in the usual way; and since the plasma response to the electromagnetic field is contained in the plasma current, we thus obtain a self-consistent set of equations governing the interaction of plasma and wave fields. The dielectric tensor contains a complete description of the types of waves that can propagate in a cold plasma [*Cross*, 1988]. The references previously listed show how the tether current source term is included to obtain waves excited by a tethered system.

As we are interested in the Alfvén wings, we restrict consideration to frequencies below the ion cyclotron frequency Ω_i and use an expression from *Sanmartín and Martinez-Sanchez* [1995] for the potential for the longitudinal part of the electric field in the propagating waves

$$\phi(\mathbf{r}) = \frac{I}{\pi}\iiint \frac{d^3k\, g(\mathbf{k}) e^{i\mathbf{k}\cdot\mathbf{r}}}{\omega k_\perp^2 \left(\varepsilon_1(\omega) - \left(\frac{ck_z}{\omega}\right)^2\right)}, \tag{1}$$

where $\mathbf{r} = (x - Vt, y, z)$ with V being the tether velocity. The time dependence is contained in the exponential, and it should be understood that $\omega = k_x V$, this equality being the mathematical expression of the steady state condition.

Electric field components perpendicular to the geomagnetic field are the corresponding derivatives of the potential, while the parallel component is negligible. Magnetic field components follow directly from the electric field. This formulation, while equivalent to others previously used, emphasizes the electrostatic nature of the phenomenon of tether-induced waves. These charge-carrying waves are excited by the regions of net charge being continually created in the plasma at the terminating contactors of the tether as the plasma flows by.

Plasma motion in this frequency range is dominated by the force due to the electric field; the force of the magnetic field on the moving particles is a secondary effect. Within the dielectric model this means the physics of the plasma response is largely governed by the diagonal components of the cold-plasma dielectric tensor perpendicular to the magnetic field

$$\varepsilon_1(\omega) \approx \frac{c^2}{V_A^2} \frac{1}{1-(\omega/\Omega_i)^2}, \tag{2}$$

where V_A is the Alfvén speed and c is the speed of light; while the tethered system's excitation of the plasma is contained in the factor

$$g(\mathbf{k}) \equiv \frac{-i}{2\pi I}\iiint d^3x\, \nabla\cdot\mathbf{j}_{\text{source}} e^{-i\mathbf{k}\cdot\mathbf{x}}, \tag{3}$$

where $\mathbf{j}_{\text{source}}$ is the current density in the tethered system and I is the tether current.

We consider the case where the contactor dimension along the direction of flight $L_x \ll V/\Omega_i \approx 36$ m (in the F region of the ionosphere), a reasonable approximation. In this case, g takes a very simple form

$$g \approx \frac{1}{\pi}\sin\left(\frac{k_y' L}{2}\right) = \frac{1}{\pi}\sin\left(\frac{L}{2}\left(k_y\cos\theta - k_z\sin\theta\right)\right), \tag{4}$$

where L is the length of the tether.

For what follows it is convenient to define a number of quantities:

$$\bar{x}_i \equiv x_i \frac{\Omega_i}{V},$$

$$E_0 \equiv \frac{\Omega_i V_A}{Vc^2} I \cong 0.83\times 10^{-3} \frac{\text{Volts}}{\text{meter}} \times I(\text{A}), \quad \bar{E}_i \equiv \frac{E_i}{E_0}$$

$$\bar{Y}_{+,-} \equiv \bar{y} \pm \tfrac{1}{2}\bar{L}\cos\theta, \quad \bar{Z}_{+,-} \equiv \bar{z} \pm \tfrac{1}{2}\bar{L}\sin\theta.$$

The integrals over k_y and k_z in (1) can be carried out easily by applying residue theory to obtain the following expressions for the electric field components (for $Z > 0$):

$$\bar{E}_x = F(\bar{Y}_-, \bar{Z}_+) - F(\bar{Y}_+, \bar{Z}_-) \tag{5}$$

$$\bar{E}_y = G(\bar{Y}_-, \bar{Z}_+) - G(\bar{Y}_+, \bar{Z}_-), \tag{6}$$

where the first terms correspond to the contibutions of the top contactor, the second terms correspond to those of the bottom contactor, and

$$F(\bar{Y}, \bar{Z}) = \int_0^1 d\kappa\, \sqrt{1-\kappa^2}\, e^{-\kappa|\bar{Y}|} \sin\left(\kappa\left[\bar{x} + \bar{Z}\frac{V/V_A}{\sqrt{1-\kappa^2}}\right]\right) \tag{7}$$

$$G(\bar{Y}, \bar{Z}) = \int_0^1 d\kappa\, \sqrt{1-\kappa^2}\, e^{-\kappa|\bar{Y}|} \operatorname{sgn}(\bar{Y}) \cos\left(\kappa\left[\bar{x} + \bar{Z}\frac{V/V_A}{\sqrt{1-\kappa^2}}\right]\right). \tag{8}$$

For $\theta = 0$, these expressions reduce to the corresponding quantities derived by *Estes* [1988] (when the small contactor limit is taken). The Alfvén wings are wave packets composed of frequencies up to Ω_i. Near the tethered system they start out as rather compact structures with significant fields and currents largely confined to regions within a hundred meters or so of the contactors (for the small

contactors we are considering). However, as they travel away from the system, the wings progressively lose their coherence because wave components of different frequencies have different phase velocites, a consequence of expression (2). The leading edges of the wings become progressively sharper, while "ripples" in the wake become more extensive and attain greater amplitudes [*Estes*, 1988].

The fields obtained above in (5)-(8) can be evaluated by numerical integration. This can be time-consuming without necessarily being illuminating, however. There is considerable virtue in having approximate expressions that are more easily understood and which elucidate the general behavior of the solutions, particularly, if they are easier to calculate. We now obtain such useful asymptotic approximations in two different domains far from the tethered system.

Alfvén Front Structure

Let us first consider the far field near the leading edge of the wings, which is of primary interest from the standpoint of experimental measurement. This is defined by the conditions that $|\bar{x}|$ is very large, while

$$(V/V_A)\bar{Z}/|\bar{x}| \cong 1 . \tag{9}$$

Far from the tether, components with $\omega << \Omega_i$ ($\kappa<<1$) dominate in this region. Thus we take

$$\kappa\left(\bar{x}+\bar{Z}\frac{V/V_A}{\sqrt{1-\kappa^2}}\right) \cong \kappa\left(\bar{x}+(V/V_A)\bar{Z}\left(1+\tfrac{1}{2}\kappa^2\right)\right)$$
$$\cong \kappa\left(\bar{x}+(V/V_A)\bar{Z}\right)+\tfrac{1}{2}\kappa^3|\bar{x}| \tag{10}$$

in the arguments in (7) and (8). Neglecting κ^2 in the square root factor, we make the substitutions

$$s \equiv \left(\tfrac{3}{2}|\bar{x}|\right)^{\frac{1}{3}}\kappa \qquad \zeta \equiv \frac{\bar{x}+(V/V_A)\bar{Z}}{\left(\tfrac{3}{2}|\bar{x}|\right)^{\frac{1}{3}}} \tag{11}$$

and extend the upper limit of the s integration to infinity, which we justify by the assumption of large $|\bar{x}|$ and the highly oscillatory integrand, to obtain

$$F \cong \left(\tfrac{3}{2}|\bar{x}|\right)^{-\frac{1}{3}}\int_0^\infty ds\ \exp\left(\frac{-s|\bar{Y}|}{\left(\tfrac{3}{2}|\bar{x}|\right)^{\frac{1}{3}}}\right)\sin\left(\zeta s+\tfrac{1}{3}s^3\right) \tag{12}$$

$$G \cong \left(\tfrac{3}{2}|\bar{x}|\right)^{-\frac{1}{3}}\int_0^\infty ds\ \exp\left(\frac{-s|\bar{Y}|}{\left(\tfrac{3}{2}|\bar{x}|\right)^{\frac{1}{3}}}\right)\mathrm{sgn}\left(\bar{Y}\right)\cos\left(\zeta s+\tfrac{1}{3}s^3\right). \tag{13}$$

In the plane of the top or bottom Alfvén wing (i.e., for $\bar{Y} \to 0$) we have simply

$$G \cong \left(\tfrac{3}{2}|\bar{x}|\right)^{-\frac{1}{3}}\mathrm{sgn}\left(\bar{Y}\right)\int_0^\infty ds\ \cos\left(\zeta s+\tfrac{1}{3}s^3\right) = \left(\tfrac{3}{2}|\bar{x}|\right)^{-\frac{1}{3}}\pi\,\mathrm{sgn}\left(\bar{Y}\right)\mathrm{Ai}(\zeta) \tag{14}$$

Ai is one of the Airy integrals [*Abramowitz and Stegun*, 1964, pp. 446-448]. A similar expression holds true for F and the Airy integral Gi.

$$F \cong \left(\tfrac{3}{2}|\bar{x}|\right)^{-\frac{1}{3}}\int_0^\infty ds\ \sin\left(\zeta s+\tfrac{1}{3}s^3\right) = \left(\tfrac{3}{2}|\bar{x}|\right)^{-\frac{1}{3}}\pi\,\mathrm{Gi}(\zeta) \tag{15}$$

This asymptotic behavior is a feature common to other wavefronts [see, e.g., *Sanmartín and Lam*, 1971]. A transition toward this behavior can be seen already in the figures of *Estes* [1988] displaying fields and currents for points too near the tether to be in the asymptotic region.

Figure 2 displays a comparison between the values of $\bar{E}_y$ obtained by numerical integration of expression (8) and the approximation of expression (14) for points in the top Alfvén wing some 283 km away from the top contactor. Agreement is seen to be quite good for a distance of about 2 km along the x axis. The "exact" solution decays with x more rapidly than the approximation. Even beyond the region of good agreement the approximation continues to provide a useful qualitative picture of the variation in the field component in the plane of the wing. Thus the approximation does all we ask of it in terms of accuracy. It also succeeds in the area of speed and convenience. The Airy function curve in Figure 2 required seconds to generate, while the numerically integrated curve required minutes. The approximation to $\bar{E}_x$ of (15) is shown in Figure 3 for the same distance from the contactor in the top wing.

The asymptotic approximation reveals other general features of the far-field wing front. As we can see from (9), (12), and (13), the wave field amplitudes decay according to the inverse cube root of the distance along the front (i.e., $|Z|^{-\frac{1}{3}}$), although, as we have seen in the example of Figure 2, this somewhat underestimates the rate of decay as we get away from the leading edge of the wing.

Another observation we can make from the asymptotic solution is that the wings, while maintaining their general shape with increasing distance from the contactor, undergo a general broadening, that is, peaks broaden, etc. This broadening is due to the progressive loss of higher-frequency, shorter-wavelength, components, as noted by *Rasmussen et al.* [1990]. This broadening occurs pro-

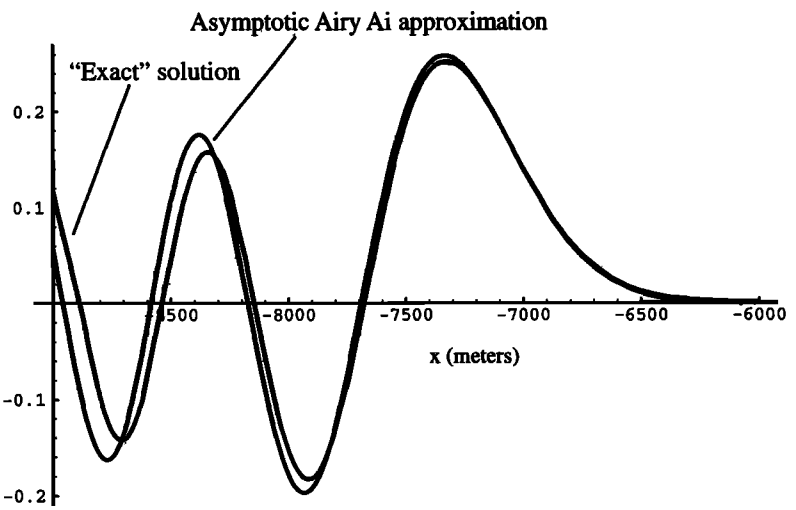

Figure 2. Comparison of asymptotic Alfvén wing solution and numerically integrated exact solution of E_y/E_0. Z_+=283 km, $E_0 \approx I(\mathrm{A})\times 10^{-3}$ Volts/m.

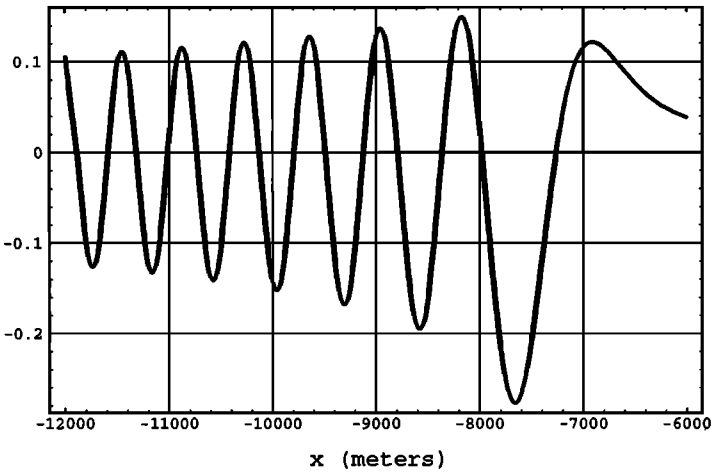

Figure 3. Asymptotic approximation to E_x/E_0 in the plane of the top Alfvén wing at a distance of 283 km from the top contactor.

portionally to the cube root of the distance along the front, which follows from the scaling of the Airy function argument defined in (11).

Rear Wing Structure

We now turn our attention to the far field well behind the wings. Although, strictly speaking, there is no well-defined back edge to the wings, *Rasmussen et al.* [1990] pointed out that far behind the leading edge of a wing, along a given ray (defined by constant Z/x) and far enough away from the contactor, only wave components close to a single well-defined frequency are found to radiate. We now obtain an asymptotic approximation appropriate to this region by applying the method of stationary phase to the integrals in expresssions (7) and (8).

This method depends upon the integrand's being highly oscillatory for large values of $|\bar{x}|$, which implies certain conditions on x/Z. Only a narrow range of κ values around the stationary point of the argument of the sinusoidal function then contributes significantly to the integral. We define $f(\kappa)$ by

$$|\bar{x}|f(\kappa) \equiv \kappa\left(\bar{x} + \bar{Z}\frac{V/V_A}{\sqrt{1-\kappa^2}}\right)$$

and look for stationary points of

$$f(\kappa) = -\kappa + \frac{\kappa V/V_A}{\sqrt{1-\kappa^2}}\bar{Z}/|\bar{x}|$$

defined by $f'(\kappa_*) = 0$, which occur for

$$1-\kappa_*^2 = \left[(V/V_A)\bar{Z}/|\bar{x}|\right]^{2/3}, \tag{16}$$

so that $f(\kappa_*) = -\kappa_*^3$, which shows the method is applicable only if $\kappa_*^3|\bar{x}| >> 1$ or

$$\left(1-\left[(V/V_A)\bar{Z}/|\bar{x}|\right]^{2/3}\right)^{3/2}|\bar{x}| >> 1. \tag{17}$$

We have further that

$$f_*'' \equiv f''(\kappa_*) = 3\kappa_*/(1-\kappa_*^2).$$

Then, in the neighborhood of the stationary point,

$$f(\kappa) \cong -\kappa_*^3 + \tfrac{1}{2}f_*''\Delta\kappa^2,$$

where $\Delta\kappa \equiv \kappa - \kappa_*$.

We change the variable of integration to

$$s \equiv \sqrt{\tfrac{1}{2}|\bar{x}|f_*''}\Delta\kappa,$$

extend the limits of integration and extract the nonoscillatory factor from the the integrand (evaluating it at the stationary point) to obtain

$$F \cong \sqrt{\frac{2}{|\bar{x}|}}\sqrt{\frac{1-\kappa_*^2}{f_*''}}e^{-\kappa_*|\bar{Y}|}\int_{-\infty}^{\infty} ds\ \sin\left(\bar{x}\kappa_*^3 + s^2\right).$$

The integral is well-known, and with substitutions we finally obtain

$$F \cong \sqrt{\frac{2\pi}{3}}\frac{\left[(V/V_A)\bar{Z}/|\bar{x}|\right]^{1/3}}{\sqrt{|\bar{x}|\kappa_*}}e^{-\kappa_*|\bar{Y}|}\sin\left(\bar{x}\kappa_*^3 + \frac{\pi}{4}\right) \tag{18}$$

for the far field behind the wings. Similarly,

$$G \cong \sqrt{\frac{2\pi}{3}}\frac{\left[(V/V_A)\bar{Z}/|\bar{x}|\right]^{1/3}}{\sqrt{|\bar{x}|\kappa_*}}e^{-\kappa_*|\bar{Y}|}\operatorname{sgn}(\bar{Y})\cos\left(\bar{x}\kappa_*^3 + \frac{\pi}{4}\right). \tag{19}$$

Rasmussen et al. [1990] applied the stationary-phase method to obtain results similar to (18)-(19) for a special tether current distribution, ignoring phase factors. They found, in particular, the amplitude along a ray of constant $|Z/x|$ to decay as the inverse square root of the distance $r = \sqrt{x^2+Z^2}$ from the contactor in the x-z plane, which agrees with our results far back in the wake. They also found the far-field, narrowband radiation around a frequency $\omega_* \equiv \kappa_*\Omega_i$ to be at an angle, defined by constant $|Z/x|$ such that our (16) was satisfied.

However, we do not agree with some of the interpretations of *Rasmussen, et al.* [1990]. They identify the region in which their stationary-phase results are valid as the "far field." Actually, a far-field analysis is valid for all $|\bar{x}| >> 1$. As we have seen, the stationary-phase results apply to only a part of the far field. Their focusing on a distance criterion for a given frequency to define what they call the far field

$$r >> \kappa_*^{-3}V_A/\Omega_i \tag{20}$$

rather obscures the decisive angle condition hidden in k_* (expressed in (20)). For small k_*, (16) implies (9), so that

$$r \cong x\frac{V_A}{V}$$

thus reducing condition (20) to our (17). However, for the region well behind the wings, where $r \sim x$, (20) becomes

$$\kappa_*^3|\bar{x}| >> V_A/V,$$

which is more stringent than necessary, according to (17).

We have obtained approximate far-field solutions for two different domains. Interestingly, and serving to confirm the results, in cases of small κ_* for which (17) is still satisfied, one can apply the stationary-phase method to (12) and (13) for the front, which is made up of all frequencies in the range

$$\left(\frac{\omega}{\Omega_i}\right)^3 \le O\left(|\bar{x}|^{-1}\right) \tag{21}$$

and use asymptotic approximations for Airy functions to obtain expressions (18) and (19).

We also note that the far front carries a negligible fraction of the Alfvén power radiated by the tether because, as already mentioned, the electric and magnetic wave components decrease as the inverse of the front thickness, and thus the Poynting-vector flux across the far front is negligible. On the other hand, one can use expressions (18) and (19) to obtain the Poynting vector S, which is along the z axis, in the region behind the fronts. The flux of S across a circular cylindrical surface parallel to the y axis and bounded by rays $Z/|x| = 0$ and $Z/|x| = V_A/V$ would yield the radiated power $I^2 Z_A$, Z_A being the radiation impedance. A straightforward integration yields

$$Z_A = \left(2V_A/c^2\right)\ln\left[2e^{\gamma-1}\left(\Omega_i L\cos\theta/V\right)\right], \quad \gamma \approx 0.577. \tag{22}$$

For vanishing geomagnetic tilt, $\theta = 0$, one recovers a result previously found by direct calculations [*Barnett and Olbert*, 1986; *Estes*, 1988; *Sanmartín and Martinez-Sanchez*, 1995].

Collisional, Short-Tether, and Thermal Effects

When ion-neutral collisions are taken into account in the cold-ion equation of motion, the diagonal components of the plasma dielectric tensor perpendicular to the geomagnetic field take the form

$$\varepsilon_1(\omega) \approx \frac{c^2}{V_A^2}\,\frac{1+i\nu_i/\omega}{1-\left(\omega+i\nu_i\right)^2/\Omega_i^2}. \tag{23}$$

At the frequencies that make up the front, which are small compared with Ω_i, the dispersion relation reads $\left(k_z V_A\right)^2 \approx \omega\left(\omega + i\nu_i\right)$, or $\mathrm{Im}\, k_z \approx \nu_i/2V_A$ for $\nu_i << \omega$. Expressions (12) and (13) must then include a factor $\exp\left(-|x|\nu_i/2V\right) \approx \exp\left(-Z\nu_i/2V_A\right)$. Thus collisions bring down the front amplitudes by 1 order of magnitude for distances along the front, $Z \approx 4V_A/\nu_i \approx 10^3$ km; taking $V_A \approx 300$ km/s and an ion-neutral collision frequency $\nu_i \approx 1$ s^{-1} for the F region of the ionophere.

At such distances the front characteristic frequency, as given by (21) with $\Omega_i = 200$ s^{-1}, is $\omega/\Omega_i \approx \left(\nu_i/4\Omega_i\right)^{1/3} << 1$. This shows that collisional decay becomes important before collisions break down the wave coherence (we have $\nu_i << \omega << \Omega_i$, as assumed).

Because of the overall exponential decay factor $\exp\left(-\kappa_*|\bar{Y}| - |x|\nu_i/2V\right)$ in (18) and (19), for long tethers one need consider the contribution of just one wing at any given point in the far field. The rate of decay κ_*, as one moves away perpendicularly from the plane of either contactor, is minimum at the front, where $\kappa_* \sim |x|^{-1/3}$; the farther along the front one moves, the slower the decay is. Collisional decay, however, grows with distance $Z \propto |x|$. At the midplane $y = 0$, that is, $|\bar{Y}_\pm| = \frac{1}{2}\bar{L}\cos\theta$, where the weakest of the top and bottom signals will be larger, the minimum of the overall decay exponent

$$\frac{L\cos\theta}{2|x|^{1/3}}\left(\Omega_i/V\right)^{2/3} + \frac{|x|\nu_i}{2V}$$

$$2\left(L\cos\theta/3V\right)^{3/4}\Omega_i^{1/2}\nu_i^{1/4}.$$

One then verifies that the top and bottom structures will be fully disjoint for

$$L\cos\theta > V/\Omega_i^{2/3}\nu_i^{1/3} \approx 2 \text{ km}. \tag{24}$$

Warm-plasma effects can be easily taken into account by considering the continuity and momentum equations and including pressure terms. Conditions $\omega = k_x V \approx kV$, $V_A >> V >>$ ion thermal velocity, and $m_i V^2 >> m_e V_A^2$ can be used to prove that such effects are negligible for frequencies not too close to Ω_i. This certainly applies at the front, and, in any case, it just excludes a narrow frequency range carrying a very small fraction of the Alfvén power that is being radiated. *McKenzie et al.* [1993] studied warm, nondispersive effects at very low frequencies.

Conclusions

We have derived integral expressions for the fields associated with the Alfvén wave packets excited by a constant-current tethered system operating in a uniform, infinite magnetoplasma with plasma parameters like those in the the F layer of the Earth's ionosphere and with the geomagnetic field perpendicular to the direction of tether motion but making an arbitrary angle with respect to the horizontal plane. Taking these integrals as a starting point, we have then obtained approximate solutions for the fields far from the tethered system in two different domains.

In the Alfvén wing front we have identified the general structure of the fields to be that of Airy functions. That is, the variation in the Alfvén wave fields along the direction of motion of the system, far from the system and in the fronts, is given by the Airy integrals Gi (for the electric field component parallel to the tether's velocity vector) and Ai (for the electric field component perpendicular to the velocity and geomagnetic field vectors). The asymptotic result also shows the Airy function amplitudes to fall off as the inverse cube root of the distance along the front and the front thickness to increase as the inverse of the amplitudes. The power carried away in the front was found to be negligible. For the far field well behind the fronts we have confirmed a previous result that in the plane of the wings, along a given ray from the contactor, the amplitude falls off as the inverse square root of the distance from the contactor, and we have obtained analytical expressions for how the field varies. We have also clarified a statement by *Rasmussen et al.* [1990] about the boundary of the far field.

Collisional decay was found to become significant at a distance of about 10^3 km from the system along the front. It was also found that the Alfvén wing structures for the top and bottom contactors were fully disjoint for tether lengths above 2 km, (the case for the 20-km, TSS-1R tether but not for the 500-m, PMG one). Thermal effects proved to be negligible.

These results could be checked through in situ measurements by properly equipped satellites. They also represent a step toward obtaining the Alfvén fields at the boundary with the atmosphere, a prerequisite for calculations of the field on the Earth's surface, which must take into account the wave reflected at the boundary The assumption of a uniform ionosphere is among the least realistic features of our model. Future work will take into account vertical variations in plasma density, collision frequencies, etc. Since the outlook for detection on the ground of the constant-current waves is not good because of the total reflection of such waves at the atmospheric boundary [*Estes*, 1989], tether currents should be pulsated at times during ground observation experiments. Future work will consider this case and the fast magnetosonic waves, which are evanescent for constant current.

Acknowledgments. The work of R. Estes was supported in part by NASA contract NAS8-36809. The work of J. Sanmartín was supported by the Comision Interministerial de Ciencia y Tecnologia of Spain under Grant PB94-0417-C03-01.

The Editor thanks D. E. Hastings and W. J. Raitt for their assistance in evaluating this paper.

References

Abramowitz, M., and I. Stegun in *Handbook of Mathematical Functions*, Dover, Mineola, N. Y., 1964.

Barnett, A., and S. Olbert, Radiation of plasma waves by a conducting body moving through a magnetized plasma, *J. Geophys. Res., 91*, 10,117, 1986.

Cross, R. in *An Introduction to Alfvén Waves*, pp. 93-99, Adam Hilger, Philadelphia, Pa., 1988.

Dobrowolny, M., and E. Melchioni, Electrodynamic aspects of the first tethered satellite mission, *J. Geophys. Res., 98*, 13,761, 1993.

Donahue, D. J., T. Neubert, and P. M. Banks, Estimating radiated power from a conducting tethered satellite system, *J. Geophys. Res., 96*, 21,245, 1991.

Drell, S. P., H. M. Foley, and M. A. Ruderman, Drag and propulsion of large satellites in the ionosphere: An Alfvén engine in space, *J. Geophys. Res., 70*, 3131, 1965.

Estes, R. D., Alfvén waves from an electrodynamic tethered satellite system, *J. Geophys. Res., 93*, 945, 1988.

Estes, R. D., Calculating the electromagnetic field on the Earth due to an electrodynamic tethered system in the ionosphere, in *Proceedings of the Third International Conference on Tethers in Space*, Am. Inst. of Aeronaut. and Astronaut., Inc., San Francisco, Calif., 1989.

Lüttgen, A., and F. M. Neubauer, Generation of plasma waves by a tethered satellite elongated in the direction of flight for arbitrary oblique geometry, *J. Geophys. Res., 99*, 23,349, 1994.

McKenzie, J. F., T. I. Woodward, and B. Inhester, Magnetoacoustic and Alfvén potentials for stationary waves in a moving plasma, *J. Geophys. Res., 98*, 9201, 1993.

Rasmussen, C. E., P. M. Banks, and K. J. Harker, The excitation of plasma waves by a current source moving in a magnetized plasma: Two-dimensional propagation, *J. Geophys. Res., 95*, 10,459, 1990.

Sanmartín, J. R., and S. H. Lam, Far-wake structure in rarefied plasma flows past charged bodies, *Phys. Fluids, 14*, 62, 1971.

Sanmartín, J. R., and M. Martinez-Sanchez, The radiation impedance of orbiting conductors, *J. Geophys. Res., 100*, 1677, 1995.

Stenzel, R. L., and J. M. Urrutia, Currents between tethered electrodes in a magnetized laboratory plasma, *J. Geophys. Res., 95*, 6209, 1990.

R. D. Estes, Harvard-Smithsonian Center for Astrophysics, Mail Stop 80, 60 Garden St., Cambridge, MA 02138. (email: restes@cfa.harvard.edu)

J. R. Sanmartín, Escuela Técnica Superior de Ingenieros Aeronáuticos, Universidad Politécnica de Madrid, 28040 Madrid, Spain. (email: jrs@faia.upm.es)

(Received November 14, 1996; revised January 30, 1997; accepted January 31, 1997.)